

Critical phenomena and phase sequence in classical bilayer Wigner crystal at zero temperature

Ladislav Šamaj* and Emmanuel Trizac

*Laboratoire de Physique Théorique et Modèles Statistiques,
UMR CNRS 8626, Université Paris-Sud, 91405 Orsay, France*

(Dated: August 21, 2018)

We study the ground-state properties of a system of identical classical Coulombic point particles, evenly distributed between two equivalently charged parallel plates at distance d ; the system as a whole is electroneutral. It was previously shown that upon increasing d from 0 to ∞ , five different structures of the bilayer Wigner crystal become energetically favored, starting from a hexagonal lattice (phase I, $d = 0$) and ending at a staggered hexagonal lattice (phase V, $d \rightarrow \infty$). In this paper, we derive new series representations of the ground-state energy for all five bilayer structures. The derivation is based on a sequence of transformations for lattice sums of Coulomb two-particle potentials plus the neutralizing background, having their origin in the general theory of Jacobi theta functions. The new series provide convenient starting points for both analytical and numerical progress. Its convergence properties are indeed excellent: Truncation at the fourth term determines in general the energy correctly up to 17 decimal digits. The accurate series representations are used to improve the specification of transition points between the phases and to solve a controversy in previous studies. In particular, it is shown both analytically and numerically that the hexagonal phase I is stable only at $d = 0$, and not in a finite interval of small distances between the plates as was anticipated before. The expansions of the structure energies around second-order transition points can be done analytically, which enables us to show that the critical behavior is of the Ginzburg-Landau type, with a mean-field critical index $\beta = 1/2$ for the growth of the order parameters.

PACS numbers: 82.70.-y, 52.27.Lw, 64.70.K-, 73.21.-b

I. INTRODUCTION

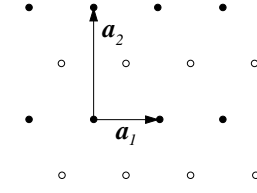
Classical charged particles, confined in a two-dimensional (2D) layer and interacting via the usual three-dimensional Coulomb potential, exhibit a crystallization into a Wigner hexagonal structure, when kinetic energy is small compared to potential energy.^{1,2} We shall be interested here in bilayer systems, that describe several properties of real physical systems in condensed and soft matter, such as semiconductors,³ quantum dots,⁴ boron nitride,⁵ laser-cooled trapped ion plasmas,⁶ dusty plasmas⁷ and colloids.⁸ For a recent review of numerical methods for quasi-2D systems with long-range interactions, see Ref.⁹ In addition, the creation of a bilayer Wigner crystal on two charged plates at some distance is of primary importance in the study of “anomalous” strong-coupling effects such as like-charge attraction or overcharging.^{10–15}

In this paper, we study the ground-state properties of a classical one-component plasma of identical Coulombic particles of the charge $-e$, evenly distributed between two plates of the same homogeneous fixed charge density σe which are at distance d . The total surface density of the particles is n , the particle density in each layer is $n_l = n/2$. The overall electroneutrality of the system is ensured by the condition $n_l = \sigma$. The phase diagram of the system at temperature $T = 0$ is determined by a single dimensionless parameter $\eta = d\sqrt{n/2} = d\sqrt{\sigma}$. By comparing the static energy of various lattices, five distinct phases were detected to be stable (providing global minimum of the energy) in different ranges of η .^{16–22} In order of increasing η , these phases are: a hexagonal lattice (I) for $\eta \in [0, \eta_1^c]$, a staggered rectangular lattice (II) for $\eta \in [\eta_1^c, \eta_2^c]$, a staggered square lattice (III) for $\eta \in [\eta_2^c, \eta_3^c]$, a staggered rhombic lattice (IV) for $\eta \in [\eta_3^c, \eta_4^c]$ and a staggered hexagonal lattice (V) for $\eta \in [\eta_4^c, \infty]$; although we use an index c in η^c , the transition point η^c from one structure to the other is not necessarily a critical point. The structures are pictured in Fig. 1. The different symbols correspond to particle positions on the opposite surfaces. The primitive translation vectors of the Bravais lattice on one of the surfaces are denoted by \mathbf{a}_1 and \mathbf{a}_2 .

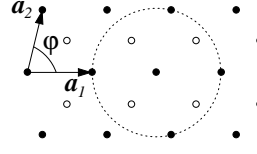
The ground-state structures I, III and V are “rigid”, i.e. they have fixed (η -independent) primary cells within their region of stability. The structures II and IV are “soft”, i.e. the shape of their primary cells is varying with increasing η , within their region of stability. We now outline the basic characteristics of the structures.^{16–22}

- **Structures I, II and III:** Within one single layer, the structure corresponds to a rectangular lattice with the aspect ratio $\Delta = |\mathbf{a}_2|/|\mathbf{a}_1|$. The equivalent structures on the two layers are shifted with respect to one another by a half period, i.e. by $(\mathbf{a}_1 + \mathbf{a}_2)/2$.

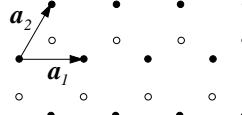
Structure I with $\Delta = \sqrt{3}$ arises naturally in the simple limit $\eta \rightarrow 0$, where the bilayer structure reduces to a single layer, which is known to crystallize in a hexagonal (equilateral triangular) lattice.^{23,24} An open question is



Structures I, II, III



Structure IV



Structure V

FIG. 1. Ground-state structures I–V of counter-ions on two parallel equivalently and homogeneously charged plates. Open and filled symbols correspond to particle positions on the opposite surfaces. The primitive translation vectors of the Bravais lattice on one of the surfaces are denoted by \mathbf{a}_1 and \mathbf{a}_2 . For structures I, II and III, we define the aspect ratio as $\Delta = |\mathbf{a}_1|/|\mathbf{a}_2|$, so that $\Delta = \sqrt{3}$ with structure I, $1 < \Delta < \sqrt{3}$ for structure II and $\Delta = 1$ for structure III. The dashed circle for structure IV is a guide to the eye, for identifying those points that are equidistant to the ion in the circle center. For a more detailed description of the structures, see the text.

whether phase I (with the fixed aspect ratio $\Delta = \sqrt{3}$) exists only at $\eta = 0$ or is stable also in a finite interval $[0, \eta_1^c]$ with some $\eta_1^c > 0$. Some numerical calculations indicate very small, but nonzero values of $\eta_1^c = 0.006$ (Ewald technique¹⁸) and 0.028 (Monte Carlo simulations²⁰). On the other hand, another study for Yukawa bilayers in the limit of infinite screening length indicates that $\eta_1^c = 0$, so that a buckled phase of type II preempts structure I when η is small but non vanishing.²¹

Structure II continuously interpolates between the rigid structures I and III. The value of the aspect ratio Δ then changes smoothly from $\sqrt{3}$ at η_1^c (phase I) to 1 at the transition point η_2^c to phase III. It is not clear whether or not η_1^c , zero or nonzero, is a standard transition point between phases I and II. The transition between phases II and III is continuous (of second order).

- The structure IV is characterized by an angle θ between primitive cell vectors \mathbf{a}_1 and \mathbf{a}_2 of the same length a . Increasing η , the angle φ changes continuously from $\pi/2$ at η_3^c (continuous transition between phases III and IV) up to η_4^c , where it drops to $\pi/3$. Together with an additional shift between the sub-lattices on the two layers, this corresponds to a discontinuous (first order) transition to phase V.
- The presence of structure V is expected for large enough $\eta \geq \eta_4^c$: At large separation between the layers, the two particle sub-lattices are only weakly coupled and so two staggered hexagonal lattices form the stable structure.

In this paper, we derive new series representations of the energy for all five bilayer structures. The derivation is based on a sequence of transformations for lattice sums of Coulomb potentials plus the neutralizing background, having their origin in the general theory of Jacobi theta functions.²⁵ The series has excellent convergence properties, which is convenient for numerical investigations, but is also conducive to analytical progress. It will be used to improve the specification of transition points between the phases and to solve the aforementioned controversy concerning the stability of phase I. In particular, it is shown both analytically and numerically that phase I is realized only at $\eta = 0$, i.e. $\eta_1^c = 0$. The expansions of the structure energies around second-order transition points can be done analytically which enables us to derive the critical exponents at phase transition points. The critical behavior is of the Ginzburg-Landau type,²⁶ with the mean-field critical index $\beta = 1/2$ for the growth of the order parameters. A preliminary account of this work has appeared in Ref.²⁷

The paper is organized as follows. Sec. II is devoted to a detailed derivation of the series representation of the energy for structures I–III. The existence of phase I at $\eta = 0$ only is established analytically and illustrated numerically. The second-order phase transition between phases II and III is then described. The energy of structure IV and the second-order phase transition between phases III and IV are treated in Sec. III. Sec. IV deals with structure V and the first-order phase transition between phases IV and V, while our conclusions are finally presented in Sec. V.

II. PHASES I-III

Structures I, II and III are treated on equal footings by considering the general case of structure II, see Fig. 1. For one single layer, the 2D lattice points are indexed by $j\mathbf{a}_1 + k\mathbf{a}_2$, where j, k are any two integers (positive, negative or zero) and

$$\mathbf{a}_1 = a(1, 0), \quad \mathbf{a}_2 = a(0, \Delta) \quad \text{with } a = \frac{1}{\sqrt{\sigma\Delta}} \quad (1)$$

are the primitive translation vectors of the Bravais lattice. The lattice spacing a is determined by the electroneutrality condition $n_l = \sigma$ with the one-layer particle density $n_l = 1/(\Delta a^2)$. The aspect ratio Δ is a continuous parameter in the interval $[1, \sqrt{3}]$; as was already mentioned, the limiting cases $\sqrt{3}$ and 1 correspond to the phases I and III, respectively.

A. Energy of phases I-III

The dielectric constant of the medium is set to unity for simplicity, and we start by a preliminary remark, valid for all phases. Our goal is to compute the total electrostatic energy, including particle-particle, particle-plate, and plate-plate interactions. The latter two contributions per unit surface can be derived straightforwardly, and respectively read $4\pi\sigma^2 e^2 d$ and $-2\pi\sigma^2 e^2 d$. The sum of both, $2\pi\sigma^2 e^2 d$, thus gives 1/2 of the particle-plate energy, and this is why in the subsequent analysis, we shall add to the non trivial particle-particle energy one half of the particle-plate energy (also referred to as the particle-background term). The resulting sum provides the full energy of the system.

The energy per particle E of the bilayer system consists of the intralayer and interlayer contributions,

$$E = E_{\text{intra}} + E_{\text{inter}}. \quad (2)$$

We first consider the intralayer contribution. It is well known that lattice sums involving the pair Coulomb interactions exhibit infinities which are canceled exactly by the neutralizing background term.^{9,28} To maintain mathematical rigor, we first restrict ourselves to a disk of finite radius R around a reference particle localized at the origin $(0, 0)$. The interaction energy due to the discrete Wigner crystal is given by

$$\frac{e^2}{2a} \sum_{\substack{j,k \\ (j,k) \neq (0,0)}} \frac{1}{\sqrt{j^2 + k^2 \Delta^2}}, \quad j^2 + k^2 \Delta^2 \leq \left(\frac{R}{a}\right)^2. \quad (3)$$

Hereinafter, the omission of the lower and upper values for integer indices j, k automatically means a summation from $-\infty$ to ∞ . The interaction of the reference particle with the 2D charge background in the disk is expressed as

$$-\frac{\sigma e^2}{2} \int_0^R d^2\mathbf{r} \frac{1}{|\mathbf{r}|} = -\frac{e^2}{2a\Delta} \int_0^{R/a} dr 2\pi r \frac{1}{r}. \quad (4)$$

E_{intra} is the sum of (3) plus (4). We intend to rewrite E_{intra} by using the gamma identity

$$\frac{1}{\sqrt{z}} = \frac{1}{\sqrt{\pi}} \int_0^\infty \frac{dt}{\sqrt{t}} e^{-zt}, \quad z > 0, \quad (5)$$

a common procedure in the field.^{9,28} Each term $1/(j^2 + k^2 \Delta^2)^{1/2}$ in (3) can consequently be written as

$$\frac{1}{\sqrt{j^2 + k^2 \Delta^2}} = \frac{1}{\sqrt{\pi}} \int_0^\infty \frac{dt}{\sqrt{t}} e^{-tj^2} e^{-t\Delta^2 k^2}. \quad (6)$$

As concerns the background contribution (4), the application of the identity (5) to the term $1/r = 1/\sqrt{r^2}$ under integration leads to

$$\int_0^{R/a} dr 2\pi r \frac{1}{r} = \int_0^{R/a} dr 2\pi r \frac{1}{\sqrt{\pi}} \int_0^\infty \frac{dt}{\sqrt{t}} e^{-tr^2} = \frac{1}{\sqrt{\pi}} \int_0^\infty \frac{dt}{\sqrt{t}} \frac{\pi}{t} \left[1 - e^{-t(R/a)^2}\right]. \quad (7)$$

Altogether, we get

$$E_{\text{intra}} = \frac{e^2}{2a\sqrt{\pi}} \int_0^\infty \frac{dt}{\sqrt{t}} \left\{ \sum_{j,k} e^{-tj^2} e^{-t\Delta^2 k^2} - 1 - \frac{\pi}{t\Delta} \left[1 - e^{-t(R/a)^2}\right] \right\}, \quad j^2 + k^2 \Delta^2 \leq \left(\frac{R}{a}\right)^2. \quad (8)$$

Here, the subtraction of unity is due to the absence of the term $(j, k) = (0, 0)$ in the sum (3). Having all contributions under the same integration, we are allowed to take the limit $R/a \rightarrow \infty$, which removes the exponentially small term $\exp[-t(R/a)^2]$ and the disk constraint for lattice indices. Using the definition of the Jacobi theta function with zero argument²⁹ $\theta_3(q) = \sum_j q^{j^2}$ and making the substitution $t\Delta \rightarrow t$, we end up with the result

$$\frac{E_{\text{intra}}}{e^2\sqrt{n}} = \frac{1}{2^{3/2}\sqrt{\pi}} \int_0^\infty \frac{dt}{\sqrt{t}} \left[\theta_3(e^{-t\Delta})\theta_3(e^{-t/\Delta}) - 1 - \frac{\pi}{t} \right]. \quad (9)$$

We shall repeatedly use the Poisson summation formula

$$\sum_{j=-\infty}^\infty e^{-(j+\phi)^2 t} = \sqrt{\frac{\pi}{t}} \sum_{j=-\infty}^\infty e^{2\pi i j \phi} e^{-(\pi j)^2/t}. \quad (10)$$

The asymptotic behaviors

$$\theta_3(e^{-t}) \underset{t \rightarrow 0}{\sim} \sqrt{\frac{\pi}{t}} \left(1 + 2e^{-\pi^2/t} + \dots \right), \quad \theta_3(e^{-t}) \underset{t \rightarrow \infty}{\sim} 1 + 2e^{-t} + \dots \quad (11)$$

follow immediately. We see that the background charge contribution $-\pi/t$ correctly cancels the $t \rightarrow 0$ singularity of the product of two θ_3 functions inside the square bracket in (9) and the integral converges.

The Wigner lattices on the opposite layers are shifted with respect to one another by the vector $(\mathbf{a}_1 + \mathbf{a}_2)/2$, see Fig. 1. To obtain the interlayer contribution to the energy, we first consider the disk of radius R around the (perpendicular) image of the reference particle on the opposite layer. The interaction energy of the Wigner crystal is given by

$$\frac{e^2}{2a} \sum_{j,k} \frac{1}{\sqrt{(j - \frac{1}{2})^2 + (k - \frac{1}{2})^2 \Delta^2 + (d/a)^2}}, \quad \left(j - \frac{1}{2} \right)^2 + \left(k - \frac{1}{2} \right)^2 \Delta^2 \leq \left(\frac{R}{a} \right)^2. \quad (12)$$

The interaction with the background charge is described by

$$-\frac{\sigma e^2}{2} \int_0^R d^2\mathbf{r} \frac{1}{|\mathbf{r} + \mathbf{d}|} = -\frac{e^2}{2a\Delta} \int_0^{R/a} dr 2\pi r \frac{1}{\sqrt{r^2 + (d/a)^2}}. \quad (13)$$

Proceeding as in the previous case and taking into account that $d/a = \eta\sqrt{\Delta}$, we find

$$\frac{E_{\text{inter}}}{e^2\sqrt{n}} = \frac{1}{2^{3/2}\sqrt{\pi}} \int_0^\infty \frac{dt}{\sqrt{t}} e^{-\eta^2 t} \left[\theta_2(e^{-t\Delta})\theta_2(e^{-t/\Delta}) - \frac{\pi}{t} \right] \quad (14)$$

with the Jacobi theta function $\theta_2(q) = \sum_j q^{(j-\frac{1}{2})^2}$. It follows from Eq. (10) that

$$\theta_2(e^{-t}) \underset{t \rightarrow 0}{\sim} \sqrt{\frac{\pi}{t}} \left(1 - 2e^{-\pi^2/t} + \dots \right), \quad \theta_2(e^{-t}) \underset{t \rightarrow \infty}{\sim} 2e^{-t/4} + \dots, \quad (15)$$

so that the integral in Eq. (14) converges, as it should.

The total energy per particle E reads

$$\frac{E(\Delta, \eta)}{e^2\sqrt{n}} = \frac{1}{2^{3/2}\sqrt{\pi}} \int_0^\infty \frac{dt}{\sqrt{t}} \left\{ \left[\theta_3(e^{-t\Delta})\theta_3(e^{-t/\Delta}) - 1 - \frac{\pi}{t} \right] + e^{-\eta^2 t} \left[\theta_2(e^{-t\Delta})\theta_2(e^{-t/\Delta}) - \frac{\pi}{t} \right] \right\}. \quad (16)$$

Note the invariance of E with respect to the transformation $\Delta \rightarrow 1/\Delta$, which is physically clear from the configuration sketched in Fig 1 (label exchange of the two Bravais vectors \mathbf{a}_1 and \mathbf{a}_2). From a numerical point of view, there are two “dangerous” limits: $t \rightarrow 0$ and $t \rightarrow \infty$, that jeopardize accuracy. To simplify the integral representation of E , we split the range of integration into two parts, $[0, \pi]$ and $[\pi, \infty]$, and transform the integral over $[\pi, \infty]$ to the one over $[0, \pi]$ by using the Poisson formula (10). For the term containing the product of two θ_3 functions, the procedure reads

$$\int_\pi^\infty \frac{dt}{\sqrt{t}} \left[\theta_3(e^{-t\Delta})\theta_3(e^{-t/\Delta}) - 1 - \frac{\pi}{t} \right] \equiv \int_\pi^\infty \frac{dt}{\sqrt{t}} \left[\sum_j e^{-tj^2\Delta} \sum_k e^{-tk^2/\Delta} - 1 - \frac{\pi}{t} \right]$$

$$\begin{aligned}
&= \int_{\pi}^{\infty} \frac{dt}{\sqrt{t}} \left[\frac{\pi}{t} \sum_j e^{-(\pi j)^2/(\Delta t)} \sum_k e^{-(\pi k)^2 \Delta/t} - 1 - \frac{\pi}{t} \right] \\
&= \int_0^{\pi} \frac{\pi dt'}{(t')^{3/2}} \left[\frac{t'}{\pi} \sum_j e^{-t' j^2/\Delta} \sum_k e^{-t' k^2 \Delta} - 1 - \frac{t'}{\pi} \right] \\
&\equiv \int_0^{\pi} \frac{dt}{\sqrt{t}} \left[\theta_3(e^{-t\Delta}) \theta_3(e^{-t/\Delta}) - 1 - \frac{\pi}{t} \right]. \tag{17}
\end{aligned}$$

Here, going from the third integral to the fourth one, we applied the substitution $t' = \pi^2/t$. Similarly, we have

$$\begin{aligned}
\int_{\pi}^{\infty} \frac{dt}{\sqrt{t}} e^{-\eta^2 t} \left[\theta_2(e^{-t\Delta}) \theta_2(e^{-t/\Delta}) - \frac{\pi}{t} \right] &\equiv \int_{\pi}^{\infty} \frac{dt}{\sqrt{t}} e^{-\eta^2 t} \left[\sum_j e^{-t(j-\frac{1}{2})^2 \Delta} \sum_k e^{-t(k-\frac{1}{2})^2/\Delta} - \frac{\pi}{t} \right] \\
&= \int_{\pi}^{\infty} \frac{dt}{\sqrt{t}} e^{-\eta^2 t} \left[\frac{\pi}{t} \sum_j (-1)^j e^{-(\pi j)^2/(\Delta t)} \sum_k (-1)^k e^{-(\pi k)^2 \Delta/t} - \frac{\pi}{t} \right] \\
&= \int_0^{\pi} \frac{\pi dt'}{(t')^{3/2}} e^{-(\pi \eta)^2/t'} \left[\frac{t'}{\pi} \sum_j (-1)^j e^{-t' j^2/\Delta} \sum_k (-1)^k e^{-t' k^2 \Delta} - \frac{t'}{\pi} \right] \\
&\equiv \int_0^{\pi} \frac{dt}{\sqrt{t}} e^{-(\pi \eta)^2/t} \left[\theta_4(e^{-t\Delta}) \theta_4(e^{-t/\Delta}) - 1 \right], \tag{18}
\end{aligned}$$

where the Jacobi theta function $\theta_4(q) = \sum_j (-1)^j q^{j^2}$. The asymptotic behaviors

$$\theta_4(e^{-t}) \underset{t \rightarrow 0}{\sim} \sqrt{\frac{\pi}{t}} e^{-\pi^2/(4t)} + \dots, \quad \theta_4(e^{-t}) \underset{t \rightarrow \infty}{\sim} 1 - 2e^{-t} + \dots \tag{19}$$

ensure the convergence of the resulting integral. To summarize this paragraph, the total energy (16) can be rewritten as an integral over the finite interval $[0, \pi]$ as follows

$$\begin{aligned}
\frac{E(\Delta, \eta)}{e^2 \sqrt{n}} &= \frac{1}{2^{3/2} \sqrt{\pi}} \int_0^{\pi} \frac{dt}{\sqrt{t}} \left\{ 2 \left[\theta_3(e^{-t\Delta}) \theta_3(e^{-t/\Delta}) - 1 - \frac{\pi}{t} \right] \right. \\
&\quad \left. + e^{-\eta^2 t} \left[\theta_2(e^{-t\Delta}) \theta_2(e^{-t/\Delta}) - \frac{\pi}{t} \right] + e^{-(\pi \eta)^2/t} \left[\theta_4(e^{-t\Delta}) \theta_4(e^{-t/\Delta}) - 1 \right] \right\}. \tag{20}
\end{aligned}$$

The exact cancellation of singular terms near $t = 0$ in this expression for E represents a numerical obstacle that should be circumvented. To accomplish the cancellation analytically, we shall consider the series representations of Jacobi theta functions and apply to them the Poisson transformation formula (10); after subtracting explicitly the singular term, the result appears as a series of special functions. In particular, for the first term in the integral (20) we obtain

$$\begin{aligned}
\int_0^{\pi} \frac{dt}{\sqrt{t}} \left[\theta_3(e^{-t\Delta}) \theta_3(e^{-t/\Delta}) - 1 - \frac{\pi}{t} \right] &= \int_0^{\pi} \frac{dt}{\sqrt{t}} \left[\sum_{j,k} e^{-tj^2 \Delta} e^{-tk^2/\Delta} - \frac{\pi}{t} \right] - 2\sqrt{\pi} \\
&= \int_0^{\pi} dt \frac{\pi}{t^{3/2}} \left[\sum_{j,k} e^{-(\pi j)^2/(\Delta t)} e^{-(\pi k)^2 \Delta/t} - 1 \right] - 2\sqrt{\pi}. \tag{21}
\end{aligned}$$

The subtraction of the singularity is equivalent to the omission of the term $(j, k) = (0, 0)$ from the summation. Using the substitution $t' = t/\pi^2$ and introducing the function

$$z_{\nu}(x, y) = \int_0^{1/\pi} \frac{dt}{t^{\nu}} e^{-xt} e^{-y/t} \quad \text{for } y > 0, \tag{22}$$

the last expression in Eq. (21) can be written as

$$2 \sum_{j=1}^{\infty} [z_{3/2}(0, j^2/\Delta) + z_{3/2}(0, j^2 \Delta)] + 4 \sum_{j,k=1}^{\infty} z_{3/2}(0, j^2/\Delta + k^2 \Delta) - 2\sqrt{\pi}. \tag{23}$$

Finally, performing the above procedure for all terms under integration in (20), we end up with the series representation

$$\begin{aligned} \frac{E(\Delta, \eta)}{e^2 \sqrt{n}} = & \frac{1}{2^{3/2} \sqrt{\pi}} \left\{ 4 \sum_{j=1}^{\infty} [z_{3/2}(0, j^2/\Delta) + z_{3/2}(0, j^2 \Delta)] + 8 \sum_{j,k=1}^{\infty} z_{3/2}(0, j^2/\Delta + k^2 \Delta) \right. \\ & + 2 \sum_{j=1}^{\infty} (-1)^j [z_{3/2}((\pi\eta)^2, j^2/\Delta) + z_{3/2}((\pi\eta)^2, j^2 \Delta)] + 4 \sum_{j,k=1}^{\infty} (-1)^j (-1)^k z_{3/2}((\pi\eta)^2, j^2/\Delta + k^2 \Delta) \\ & \left. + 4 \sum_{j,k=1}^{\infty} z_{3/2}(0, \eta^2 + (j-1/2)^2/\Delta + (k-1/2)^2 \Delta) - 4\sqrt{\pi} - \pi z_{1/2}(0, \eta^2) \right\}. \end{aligned} \quad (24)$$

The function $z_\nu(x, y)$ with $x = 0$ is related to the so-called Misra function^{30,31} which was extensively used in single-layer lattice summations.^{32,33} For our bilayer system with positive η we need the more general function (22) with $x \geq 0$. The convergence properties of our series can be anticipated from the asymptotic relation $z_\nu(0, y) \sim e^{-\pi y} \pi^{\nu-2}/y$.

In numerical calculations, for a given η we have to find such Δ^* which provides the minimum value of the energy (24). In practice, the series (24) must be cut at some $j, k = M$. We document excellent convergence properties of the series (24) by considering the single-layer case ($\Delta = \sqrt{3}, \eta = 0$) for which the exact³⁴

$$E(\sqrt{3}, 0)/(e^2 \sqrt{n}) = -1.96051578931989165 \dots \quad (25)$$

The cut at $M = 1, 2, 3, 4$ reproduces this exact value up to 2, 5, 10, 17 decimal digits, respectively. A similar accuracy is reached in all considered cases. To be extremely accurate, we apply the $M = 5$ cut everywhere, and use the *Mathematica* software.

Another advantage of the series representation (24) is the possibility of an explicit expansion of the function $E(\Delta^*, \eta)/(e^2 \sqrt{n})$ around the controversial point $\eta = 0$ and around the critical point η_c^2 . As will be shown, this requires an analogous Taylor expansion of our z -functions.

B. Going from phase I to phase II

We know^{23,24} that for the single layer, i.e. $\eta = 0$, the structure providing the minimum of the energy is the hexagonal lattice with $\Delta = \sqrt{3}$. In what follows, we shall investigate the minimum of the energy (24) in the neighborhood of the point $(\Delta = \sqrt{3}, \eta = 0)$. We set $\Delta = \sqrt{3} - \epsilon$ and consider ϵ to be infinitesimally small. To derive a small- ϵ expansion of the energy (24), we first perform this task for its series components. From the integral definition (22) it is easy to show that the z -functions under consideration exhibit an analytic (Taylor) expansion in ϵ of the form

$$z_{3/2}(0, j^2 \Delta) = z_{3/2}(0, j^2 \sqrt{3}) + \epsilon j^2 z_{5/2}(0, j^2 \sqrt{3}) + \frac{1}{2} \epsilon^2 j^4 z_{7/2}(0, j^2 \sqrt{3}) + \mathcal{O}(\epsilon^3), \quad (26)$$

$$z_{3/2}(0, j^2/\Delta) = z_{3/2}(0, j^2/\sqrt{3}) - \epsilon \frac{j^2}{3} z_{5/2}(0, j^2/\sqrt{3}) + \epsilon^2 \left[\frac{j^4}{18} z_{7/2}(0, j^2/\sqrt{3}) - \frac{j^2}{3^{3/2}} z_{5/2}(0, j^2/\sqrt{3}) \right] + \mathcal{O}(\epsilon^3), \quad (27)$$

$$\begin{aligned} z_{3/2}(0, j^2/\Delta + k^2 \Delta) = & z_{3/2}(0, j^2/\sqrt{3} + k^3 \sqrt{3}) + \epsilon \left(k^2 - \frac{j^2}{3} \right) z_{5/2}(0, j^2/\sqrt{3} + k^2 \sqrt{3}) \\ & + \epsilon^2 \left[\frac{1}{2} \left(k^2 - \frac{j^2}{3} \right)^2 z_{7/2}(0, j^2/\sqrt{3} + k^2 \sqrt{3}) - \frac{j^2}{3^{3/2}} z_{5/2}(0, j^2/\sqrt{3} + k^2 \sqrt{3}) \right] + \mathcal{O}(\epsilon^3). \end{aligned} \quad (28)$$

Similar expansions can be derived for $z_{3/2}((\pi\eta)^2, j^2 \Delta)$, $z_{3/2}((\pi\eta)^2, j^2/\Delta)$, etc. Inserting these expansions into (24), we obtain

$$\frac{E(\sqrt{3} - \epsilon, \eta)}{e^2 \sqrt{n}} = \frac{E(\sqrt{3}, \eta)}{e^2 \sqrt{n}} + f_1(\eta) \epsilon + f_2(\eta) \epsilon^2 + \mathcal{O}(\epsilon^3), \quad (29)$$

where the explicit form of the prefactor functions $f_1(\eta)$ and $f_2(\eta)$ is written in the Appendix.

Being close to the point $(\Delta = \sqrt{3}, \eta = 0)$, we are interested in the small- η behavior of the functions $f_1(\eta)$ and $f_2(\eta)$. The corresponding Taylor expansions in powers of η^2 can be performed explicitly, too. The explicit form of $E(\sqrt{3}, \eta)$ is here immaterial. We find that $f_1(0) = 0$, and, with a high precision,

$$f_1(\eta) = -0.5833059875 \dots \eta^2 + \mathcal{O}(\eta^4), \quad f_2(\eta) = 0.0408440789 \dots + \mathcal{O}(\eta^2). \quad (30)$$

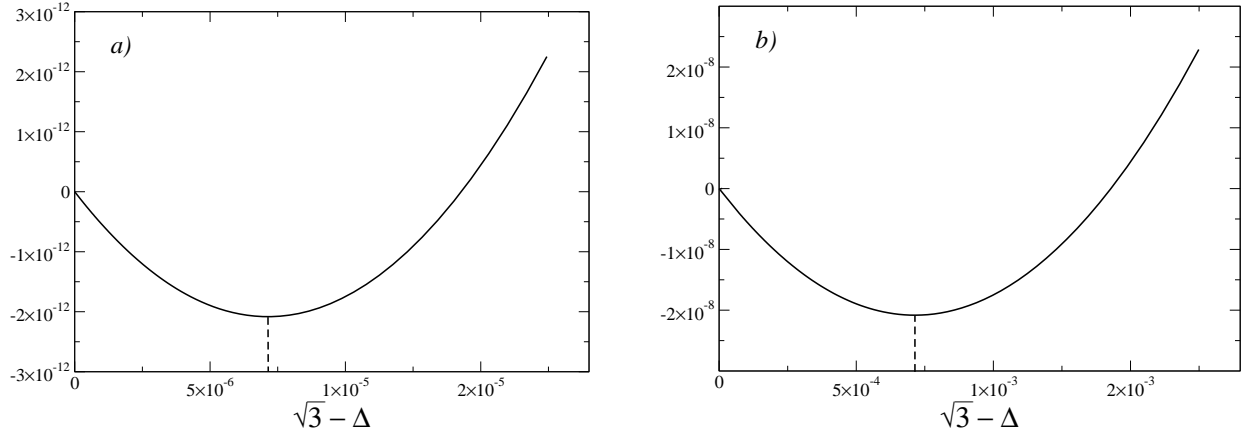


FIG. 2. The difference between the dimensionless energies $[E(\Delta, \eta) - E(\sqrt{3}, \eta)] / (e^2 \sqrt{n})$ versus $\epsilon = \sqrt{3} - \Delta$, calculated numerically by using (24) for two small values of η : a) $\eta = 10^{-3}$ and b) $\eta = 10^{-2}$. For the range of aspect ratios chosen, these curves are indistinguishable from the analytical prediction $-0.5833 \eta^2 \epsilon + 0.0408 \epsilon^2$, stemming from Eqs. (29) and (30). The values of ϵ^* , which provide the energy minimum in the asymptotic limit $\eta \rightarrow 0$ according to (32), are depicted by the vertical dashed lines for comparison.

For a fixed η , the extremum of the energy (29) appears at $\epsilon^* = \sqrt{3} - \Delta^*$ given by the stationarity condition

$$\left. \frac{\partial}{\partial \epsilon} \frac{E(\sqrt{3} - \epsilon, \eta)}{e^2 \sqrt{n}} \right|_{\epsilon = \epsilon^*} = 0 = f_1(\eta) + 2f_2(\eta)\epsilon^*. \quad (31)$$

Namely,

$$\sqrt{3} - \Delta^* \equiv \epsilon^*(\eta) = -\frac{f_1(\eta)}{2f_2(\eta)} = 7.14064 \dots \eta^2 + \mathcal{O}(\eta^4). \quad (32)$$

Since $\partial_\epsilon^2 E(\sqrt{3} - \epsilon, \eta)|_{\epsilon = \epsilon^*} = f_2(\eta) > 0$, the extremum is the minimum. The result (32) tells us that howsoever small the dimensionless distance η is, the buckled structure II with $\Delta < \sqrt{3}$ takes place. In other words, the structure I exists only strictly at $\eta_1^c = 0$. The fact that in the previous works^{18,20} the structure I was detected also for very small positive values of η is probably related to extremely small values of the deviation $\epsilon^* \propto \eta^2$ for these η 's, which are “invisible” by standard numerical methods. Like for instance, the structure I border reported in¹⁸ $\eta_1^c = 0.006$ corresponds to $\epsilon^* = 0.00026 \dots$

In Fig. 2, we present the plots of the difference between the dimensionless energies $[E(\Delta, \eta) - E(\sqrt{3}, \eta)] / (e^2 \sqrt{n})$ versus $\epsilon = \sqrt{3} - \Delta$, calculated numerically by using (24) for two very small values of η : a) $\eta = 10^{-3}$ and b) $\eta = 10^{-2}$ which are well below/above the previous estimate of the phase I threshold,¹⁸ respectively. Alternatively, using the analytical expressions (29) and (30) leads to the very same data. The nonzero values of ϵ^* , which provide the energy minima in the asymptotic limit $\eta \rightarrow 0$ according to formula (32), are depicted by the dashed lines for comparison. We see that the energy minima fit well with the expected ϵ^* which is clear evidence for the phase I instability. Note extremely small values $\propto 10^{-12} - 10^{-8}$ of the energy difference, in Fig. 2, which justifies the derivation of an accurate formula for the Coulombic energy.

In Fig. 3, the asymptotic relation (32) (dashed line) is tested against numerical minimization of the energy (24) (solid curve) for small and intermediary values of η , in the logarithmic scale. The agreement is very good, not only for small η , but in the whole range of stability of phase II (it will be shown in the next subsection that phase II border is given by $\eta_2^c \simeq 0.26276 \dots$).

C. Transition between phases II and III

Going from phase I to phase II is not a phase transition in the usual sense. However, the symmetry of the energy E with respect to the transformation $\Delta \rightarrow 1/\Delta$ has the fixed (self dual) point at $\Delta = 1$ which is the critical point of the phase transition from phase II to III. Let us parameterize Δ as follows $\Delta = \exp(\epsilon)$. The symmetry $\Delta \rightarrow 1/\Delta$ is now equivalent to $\epsilon \rightarrow -\epsilon$, i.e. the energy E is an even function of ϵ . The expansion of E around the critical point

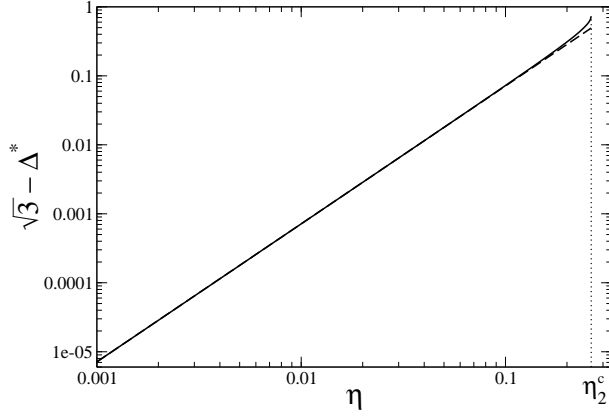


FIG. 3. Going from phase I to II: The test of the asymptotic relation (32) (dashed line) against numerical minimization of the energy (24) (solid curve) for small and intermediary values of η , in the logarithmic scale.

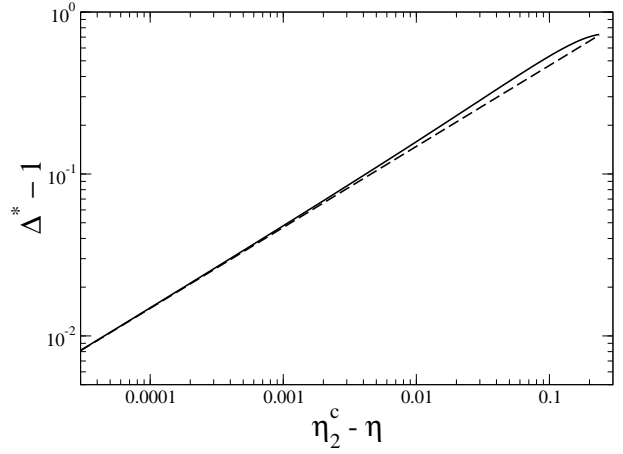


FIG. 4. Transition between phases II and III: The test of the asymptotic relation (37) (dashed line) against numerical minimization of the energy (24) (solid curve), in the logarithmic scale.

$\Delta = 1$ ($\epsilon = 0$) in small deviation ϵ follows from the representation (24):

$$\frac{E(\epsilon^\epsilon, \eta)}{e^2 \sqrt{n}} = \frac{E(1, \eta)}{e^2 \sqrt{n}} + g_2(\eta) \epsilon^2 + g_4(\eta) \epsilon^4 + \mathcal{O}(\epsilon^6). \quad (33)$$

The explicit form of $g_2(\eta)$ is written in the Appendix and $g_4(\eta)$ is not presented due to lack of space, but has been derived. The energy (33) has the Ginzburg-Landau form, ϵ being the order parameter. In contrast to that mean field theory, the expression for our energy is exact.

The critical point is associated with the vanishing of the prefactor to ϵ^2 ,

$$g_2(\eta) \Big|_{\eta=\eta_2^c} = 0, \quad \eta_2^c = 0.2627602682 \dots \quad (34)$$

The values of η_2^c obtained in the previous studies were 0.262,¹⁸ which is remarkably precise, 0.28²⁰ and 0.27.²² The functions $g_2(\eta)$ and $g_4(\eta)$ exhibit the following expansions around the critical η_2^c :

$$g_2(\eta) = -0.4620982808 \dots (\eta_2^c - \eta) + \mathcal{O}((\eta_2^c - \eta)^2), \quad g_4(\eta) = 0.1054378203 \dots + \mathcal{O}(\eta_2^c - \eta). \quad (35)$$

The extremum (minimum) of the energy (33) appears at $\epsilon^* \simeq \Delta^* - 1$ given by the condition

$$\left. \frac{\partial}{\partial \epsilon} \frac{E(\epsilon^\epsilon, \eta)}{e^2 \sqrt{n}} \right|_{\epsilon=\epsilon^*} = 0 = 2g_2(\eta) \epsilon^* + 4g_4(\eta) \epsilon^{*3}. \quad (36)$$

For $\eta < \eta_2^c$ (the “ordered” phase II), we have one trivial solution $\epsilon^* = 0$ which however provides the local maximum of the energy. There exist two conjugate nontrivial solutions which yield the needed energy minimum; considering one of these solutions, we arrive at

$$\Delta^* - 1 \simeq \epsilon^* = \left(-\frac{g_2(\eta)}{2g_4(\eta)} \right)^{1/2} \simeq 1.48031 \sqrt{\eta_2^c - \eta}. \quad (37)$$

The critical index β , describing the growth of the order parameter from its zero critical value via $\epsilon^* \propto (\eta_2^c - \eta)^\beta$, has the mean field value 1/2. In Fig. 4, in the logarithmic scale, the asymptotic relation (37) (dashed line) is compared with the numerical minimization of the energy (24) (solid curve).

For $\eta > \eta_2^c$ (the “disordered” phase III), we have the only solution to (36) $\epsilon^* = 0$ (or equivalently $\Delta^* = 1$), i.e. the rigid phase III is stable, up to a transition to phase IV discussed in the next section.

The plot of the lattice aspect ratio Δ^* versus η , obtained by the numerical minimization of the energy (24) in the whole stability range of the phase II, is pictured by the solid curve in Fig. 5. Δ^* changes from $\sqrt{3}$ at $\eta = 0$ to 1 at $\eta = \eta_2^c$. Numerical data of Goldoni and Peeters¹⁸ (open circles) are also presented for comparison. The asymptotic relations (32) for $\eta \rightarrow 0$ and (37) for $\eta \rightarrow \eta_2^c$ are also provided, for completeness.

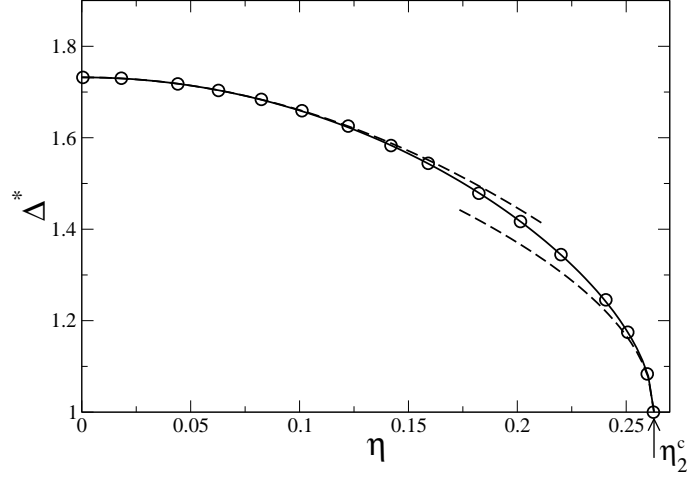


FIG. 5. The stability range of phase II: The plot of the lattice aspect ratio Δ^* versus η , obtained by the numerical minimization of the energy (24), is pictured by the solid curve. Numerical data of Ref.¹⁸ are presented by open circles. The asymptotic relations (32) for $\eta \rightarrow 0$ and (37) for $\eta \rightarrow \eta_2^c$ are depicted by dashed curves.

III. PHASE IV

In each of the two layers of phase IV (see Fig. 1), the elementary cell is the rhombus with angle φ between the primitive translation vectors

$$\mathbf{a}_1 = a(1, 0), \quad \mathbf{a}_2 = a(\cos \varphi, \sin \varphi) \quad \text{with } a = \frac{1}{\sqrt{\sigma \sin \varphi}}. \quad (38)$$

The lattice spacing a is determined by the electroneutrality condition $n_l = \sigma$; there is just one particle per rhombus of the surface $a^2 \sin \varphi$ and so $n_l = 1/(a^2 \sin \varphi)$. The special case of $\varphi = \pi/2$ corresponds to phase III.

A. Energy of phase IV

As before, the energy per particle E of the bilayer structure consists of the intralayer and interlayer contributions, $E = E_{\text{intra}} + E_{\text{inter}}$. As concerns the intralayer part, the 2D lattice vectors on one layer are indexed with respect to a reference particle on the same layer by $\mathbf{r}(j, k) = j\mathbf{a}_1 + k\mathbf{a}_2$, where j, k are any two integers except for $(0, 0)$. The square of the lattice vector can be written as

$$|\mathbf{r}(j, k)|^2 = a^2 (j^2 + k^2 + 2jk \cos \varphi) = a^2 [(j+k)^2 \cos^2(\varphi/2) + (j-k)^2 \sin^2(\varphi/2)]. \quad (39)$$

This formula represents a kind of “diagonalization” of $|\mathbf{r}(j, k)|^2$ in indices. If $j+k$ is an even integer, we introduce new indices $n = (j+k)/2$ and $m = (j-k)/2$ covering all integers except for $(n, m) \neq (0, 0)$. If $j+k$ is an odd integer, we introduce indices $n = (j+k+1)/2$ and $m = (j-k+1)/2$ covering all integers. Thus the interaction energy due to the Wigner crystal can be expressed as

$$\begin{aligned} \frac{e^2}{2a} \sum_{\substack{j,k \\ (j,k) \neq (0,0)}} \frac{1}{|\mathbf{r}(j, k)|} &= \frac{e^2}{4a} \left[\sum_{\substack{n,m \\ (n,m) \neq (0,0)}} \frac{1}{\sqrt{n^2 \cos^2(\varphi/2) + m^2 \sin^2(\varphi/2)}} \right. \\ &\quad \left. + \sum_{n,m} \frac{1}{\sqrt{(n-1/2)^2 \cos^2(\varphi/2) + (m-1/2)^2 \sin^2(\varphi/2)}} \right]. \end{aligned} \quad (40)$$

Adding to this expression the interaction with the neutralizing background and using the gamma identity (5) in close analogy with the previous section, we obtain

$$\frac{E_{\text{intra}}}{e^2 \sqrt{n}} = \frac{1}{4\sqrt{\pi}} \int_0^\infty \frac{dt}{\sqrt{t}} \left\{ \left[\theta_3(e^{-t\delta}) \theta_3(e^{-t/\delta}) - 1 - \frac{\pi}{t} \right] + \left[\theta_2(e^{-t\delta}) \theta_2(e^{-t/\delta}) - \frac{\pi}{t} \right] \right\}, \quad (41)$$

where $\delta = \tan(\varphi/2)$.

The Wigner lattices on the opposite layers are shifted with respect to one another by the vector $(\mathbf{a}_1 + \mathbf{a}_2)/2$. To determine the interlayer contribution to the energy, we first consider the square of the vector between the reference particle on one layer and the vertices of the Wigner crystal on the other layer at distance d :

$$\begin{aligned} |\mathbf{r}(j, k)|^2 &= a^2 [(j - 1/2)^2 + (k - 1/2)^2 + 2(j - 1/2)(k - 1/2) \cos \varphi] + d^2 \\ &= a^2 [(j + k - 1)^2 \cos^2(\varphi/2) + (j - k)^2 \sin^2(\varphi/2) + (d/a)^2]. \end{aligned} \quad (42)$$

Thus the interaction energy with the Wigner crystal reads

$$\begin{aligned} \frac{e^2}{2a} \sum_{j,k} \frac{1}{|\mathbf{r}(j, k)|} &= \frac{e^2}{4a} \left[\sum_{n,m} \frac{1}{\sqrt{(n - 1/2)^2 \cos^2(\varphi/2) + m^2 \sin^2(\varphi/2) + d^2/(2a)^2}} \right. \\ &\quad \left. + \sum_{n,m} \frac{1}{\sqrt{n^2 \cos^2(\varphi/2) + (m - 1/2)^2 \sin^2(\varphi/2) + d^2/(2a)^2}} \right]. \end{aligned} \quad (43)$$

Adding the background term and using the gamma identity, we find that

$$\frac{E_{\text{inter}}}{e^2 \sqrt{n}} = \frac{1}{4\sqrt{\pi}} \int_0^\infty \frac{dt}{\sqrt{t}} e^{-\eta^2 t/2} \left\{ \left[\theta_3(e^{-t\delta}) \theta_2(e^{-t/\delta}) - \frac{\pi}{t} \right] + \left[\theta_2(e^{-t\delta}) \theta_3(e^{-t/\delta}) - \frac{\pi}{t} \right] \right\}. \quad (44)$$

The total energy per particle E is the sum of (41) and (44). Note the invariance of E with respect to the transformation $\delta \rightarrow 1/\delta$. With respect to the definition of $\delta = \tan(\varphi/2)$, this symmetry is equivalent to the obvious one $\varphi \rightarrow \pi - \varphi$. Following subsequently similar lines as in previous sections, the integral range $[0, \infty]$ can be reduced to $[0, \pi]$ by using the Poisson formula (10),

$$\begin{aligned} \frac{E(\delta, \eta)}{e^2 \sqrt{n}} &= \frac{1}{4\sqrt{\pi}} \int_0^\pi \frac{dt}{\sqrt{t}} \left\{ 2 \left[\theta_3(e^{-t\delta}) \theta_3(e^{-t/\delta}) - 1 - \frac{\pi}{t} \right] + \left[\theta_2(e^{-t\delta}) \theta_2(e^{-t/\delta}) - \frac{\pi}{t} \right] + \left[\theta_4(e^{-t\delta}) \theta_4(e^{-t/\delta}) - 1 \right] \right. \\ &\quad + e^{-\eta^2 t/2} \left[\theta_3(e^{-t\delta}) \theta_2(e^{-t/\delta}) - \frac{\pi}{t} \right] + e^{-(\pi\eta)^2/(2t)} \left[\theta_3(e^{-t\delta}) \theta_4(e^{-t/\delta}) - 1 \right] \\ &\quad \left. + e^{-\eta^2 t/2} \left[\theta_2(e^{-t\delta}) \theta_3(e^{-t/\delta}) - \frac{\pi}{t} \right] + e^{-(\pi\eta)^2/(2t)} \left[\theta_4(e^{-t\delta}) \theta_3(e^{-t/\delta}) - 1 \right] \right\}. \end{aligned} \quad (45)$$

Applying again the Poisson transformation formula (10) to the series representations of Jacobi theta functions, the singular $t \rightarrow 0$ terms are canceled explicitly and we end up with the representation of the energy per particle E in terms of z -functions defined in (22):

$$\begin{aligned} \frac{E(\delta, \eta)}{e^2 \sqrt{n}} &= \frac{1}{2\sqrt{\pi}} \left\{ \sum_{j=1}^\infty [2 + (-1)^j] [z_{3/2}(0, j^2/\delta) + z_{3/2}(0, j^2\delta)] + 2 \sum_{j,k=1}^\infty [2 + (-1)^j (-1)^k] z_{3/2}(0, j^2/\delta + k^2\delta) \right. \\ &\quad + 2 \sum_{j,k=1}^\infty z_{3/2}(0, (j - 1/2)^2/\delta + (k - 1/2)^2\delta) + \sum_{j=1}^\infty [1 + (-1)^j] [z_{3/2}((\pi\eta)^2/2, j^2/\delta) + z_{3/2}((\pi\eta)^2/2, j^2\delta)] \\ &\quad + 2 \sum_{j,k=1}^\infty [(-1)^j + (-1)^k] z_{3/2}((\pi\eta)^2/2, j^2/\delta + k^2\delta) \\ &\quad + 2 \sum_{j,k=1}^\infty [z_{3/2}(0, \eta^2/2 + (j - 1/2)^2/\delta + k^2\delta) + z_{3/2}(0, \eta^2/2 + (j - 1/2)^2\delta + k^2\delta)] \\ &\quad \left. + \sum_{j=1}^\infty [z_{3/2}(0, \eta^2/2 + (j - 1/2)^2/\delta) + z_{3/2}(0, \eta^2/2 + (j - 1/2)^2\delta)] - 3\sqrt{\pi} - \pi z_{1/2}(0, \eta^2/2) \right\}. \end{aligned} \quad (46)$$

B. Transition between phases III and IV

The symmetry of the energy E with respect to the transformation $\delta \rightarrow 1/\delta$ has the fixed point at $\delta = 1$ which is the critical point of the phase transition between the phases III and IV. Parameterizing δ as $\delta \equiv \tan(\varphi/2) = \exp(-\epsilon)$,

the symmetry takes form $\epsilon \rightarrow -\epsilon$ and the energy E is an even function of ϵ . The expansion of E around the critical point $\delta = 1$ (equivalent to $\theta = \pi/2$ or $\epsilon = 0$) in small ϵ follows from the representation (46):

$$\frac{E(e^{-\epsilon}, \eta)}{e^2 \sqrt{n}} = \frac{E(1, \eta)}{e^2 \sqrt{n}} + h_2(\eta) \epsilon^2 + h_4(\eta) \epsilon^4 + \mathcal{O}(\epsilon^6). \quad (47)$$

The explicit form of $h_2(\eta)$ is presented in the Appendix; The expression for $h_4(\eta)$ is too lengthy to be given, but is at our disposal.

The critical point is associated with the vanishing of the prefactor of ϵ^2 ,

$$h_2(\eta) \Big|_{\eta=\eta_3^c} = 0, \quad \eta_3^c = 0.6214809246 \dots \quad (48)$$

The values of η_3^c obtained in the previous studies are 0.622,¹⁸ 0.59²⁰ and 0.62.²² The functions $h_2(\eta)$ and $h_4(\eta)$ exhibit the following expansions around the critical η_3^c :

$$h_2(\eta) = -0.2675826391 \dots (\eta - \eta_3^c) + \mathcal{O}((\eta - \eta_3^c)^2), \quad h_4(\eta) = 0.0863245072 \dots + \mathcal{O}(\eta - \eta_3^c). \quad (49)$$

The extremum (minimum) of the energy (47) appears at $\epsilon^* \simeq \pi/2 - \varphi^*$ given by the condition

$$\frac{\partial}{\partial \epsilon} \frac{E(e^{-\epsilon}, \eta)}{e^2 \sqrt{n}} \Big|_{\epsilon=\epsilon^*} = 0 = 2h_2(\eta) \epsilon^* + 4h_4(\eta) \epsilon^{*3}. \quad (50)$$

For $\eta < \eta_3^c$ (“disordered” phase III), we have the only solution $\epsilon^* = 0$ (or equivalently $\varphi^* = \pi/2$) which provides the energy minimum, i.e. the rigid phase III is stable. For $\eta > \eta_3^c$ (“ordered” phase IV), the trivial solution $\epsilon^* = 0$ becomes unstable. The couple of conjugate nontrivial solutions, which provide the energy minimum, implies

$$1 - \delta^* \simeq \epsilon^* \simeq \frac{\pi}{2} - \varphi^* = \left(-\frac{h_2(\eta)}{2h_4(\eta)} \right)^{1/2} \simeq 1.24494 \sqrt{\eta - \eta_3^c}. \quad (51)$$

The critical index β has again the mean field value $1/2$. In Fig. 6, in a log-log scale, the asymptotic relation (51) (dashed line) is tested against numerical minimization of the energy (46) (solid curve). In the upper inset, we show the dependence of the energy on the logarithm of the angle parameter $\delta = \tan(\varphi/2)$ for $\eta = 0.5$, where the phase III with $\delta = 1$ is stable. In the lower inset, the analogous plot is presented for $\eta = 0.7$, where the phase IV with $\delta \neq 1$ is stable; phase III corresponds in fact to a local maximum of the energy. Note the symmetry of the energy with respect to the transformation $\delta \rightarrow 1/\delta$ or, equivalently, $\ln \delta \rightarrow -\ln \delta$.

The plot of the angle parameter $\delta^* = \tan(\varphi^*/2)$ versus η , obtained by numerical minimization of the energy (24) in the whole stability range of the phase IV, is displayed by the solid curve in Fig. 7. δ^* changes from 1 at $\eta = \eta_3^c$ (transition point from phase III to IV) to $\delta^c = 0.69334 \dots$ at $\eta = \eta_4^c$ (transition point from phase IV to V, see the next section). Numerical data of Goldoni and Peeters¹⁸ (open circles) are presented for comparison. The asymptotic relation (51) for $\eta \rightarrow \eta_3^c$ is depicted by the dashed curve.

IV. PHASE V

In a single layer of the phase V (see Fig. 1), the elementary cell of the hexagonal lattice is the rhombus with the angle $\pi/3$ between the primitive translation vectors

$$\mathbf{a}_1 = a(1, 0), \quad \mathbf{a}_2 = \frac{a}{2}(1, \sqrt{3}) \quad \text{with } a = \frac{\sqrt{2}}{3^{1/4}} \frac{1}{\sqrt{\sigma}}. \quad (52)$$

The lattice spacing a follows from the electroneutrality condition $n_l = \sigma$; there is just one particle per rhombus of surface $\sqrt{3}a^2/2$, so that $n_l = 2/(\sqrt{3}a^2)$. Note that the images of vertices on the opposite layer are localized in the center of triangles and not rhombuses, as was the case of phase IV. There is no continuous way to pass from phase IV to phase V.

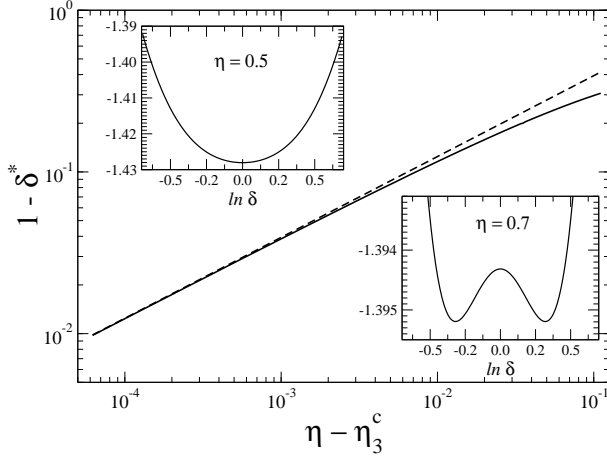


FIG. 6. Transition between phases III and IV: The test of the asymptotic relation (51) (dashed line) against a numerical minimization of the energy (46) (solid curve), in the logarithmic scale. The content of upper and lower insets is commented in the text.

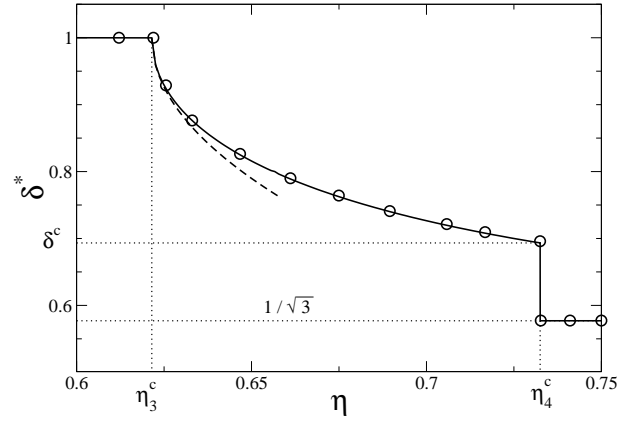


FIG. 7. Stability range of phase IV: The plot of the angle parameter δ^* versus η , obtained by the numerical minimization of the energy (46), is shown by the solid curve. Numerical data of Ref.¹⁸ are presented by open circles. The asymptotic relation (51) for $\eta \rightarrow \eta_3^c$ is depicted by the dashed curve.

A. Energy of phase V

To study the intralayer contribution to the energy of the reference particle at the origin, we first consider the Wigner crystal of lattice vectors $\mathbf{r}(j, k) = j\mathbf{a}_1 + k\mathbf{a}_2$, where integers $(j, k) \neq (0, 0)$. The square of the lattice vector is expressible as

$$|\mathbf{r}(j, k)|^2 = a^2 (j^2 + k^2 + jk) = \frac{a^2}{4} [3(j+k)^2 + (j-k)^2]. \quad (53)$$

In analogy with phase IV, we introduce new n, m indices for each of the cases $j+k$ being an even and odd integer. The interaction energy due to the Wigner crystal then reads

$$\frac{e^2}{2a} \sum_{\substack{j,k \\ (j,k) \neq (0,0)}} \frac{1}{|\mathbf{r}(j, k)|} = \frac{e^2}{2a} \left[\sum_{\substack{n,m \\ (n,m) \neq (0,0)}} \frac{1}{\sqrt{3n^2 + m^2}} + \sum_{n,m} \frac{1}{\sqrt{3(n-1/2)^2 + (m-1/2)^2}} \right]. \quad (54)$$

Adding to this expression the interaction with the neutralizing background and using the gamma identity, we find

$$\frac{E_{\text{intra}}}{e^2 \sqrt{n}} = \frac{1}{4\sqrt{\pi}} \int_0^\infty \frac{dt}{\sqrt{t}} \left\{ \left[\theta_3(e^{-t/\sqrt{3}}) \theta_3(e^{-t\sqrt{3}}) - 1 - \frac{\pi}{t} \right] + \left[\theta_2(e^{-t/\sqrt{3}}) \theta_2(e^{-t\sqrt{3}}) - \frac{\pi}{t} \right] \right\}. \quad (55)$$

The hexagonal lattices on the opposite layers are shifted with respect to one another by the vector $(\mathbf{a}_1 + \mathbf{a}_2)/3$; note that the factor $1/3$ differs from $1/2$ of the previous phases I-IV. To determine the interlayer contribution to the energy, we first consider the square of the vector between the reference particle on one layer and the vertices of the Wigner crystal on the other layer at distance d :

$$|\mathbf{r}(j, k)|^2 = a^2 [(j+1/3)^2 + (k+1/3)^2 + (j+1/3)(k+1/3)] + d^2 = \frac{a^2}{4} [3(j+k+2/3)^2 + (j-k)^2] + d^2. \quad (56)$$

Going from (j, k) to integers (n, m) , the interaction energy with the Wigner crystal on the opposite side takes the form

$$\frac{e^2}{2a} \sum_{j,k} \frac{1}{|\mathbf{r}(j, k)|} = \frac{e^2}{2a} \left[\sum_{n,m} \frac{1}{\sqrt{3(n+1/3)^2 + m^2 + (d/a)^2}} + \sum_{n,m} \frac{1}{\sqrt{3(n-1/6)^2 + (m-1/2)^2 + (d/a)^2}} \right]. \quad (57)$$

Adding the background term, using the gamma identity and the readily derivable relations

$$\sum_j e^{-3t(j+1/3)^2} = \frac{1}{2} [\theta_3(e^{-t/3}) - \theta_3(e^{-3t})], \quad \sum_j e^{-3t(j-1/6)^2} = \frac{1}{2} [\theta_2(e^{-t/3}) - \theta_2(e^{-3t})], \quad (58)$$

we find that

$$\begin{aligned} \frac{E_{\text{inter}}}{e^2\sqrt{n}} &= \frac{1}{4\sqrt{\pi}} \int_0^\infty \frac{dt}{\sqrt{t}} \left(-\frac{1}{2}e^{-\eta^2 t/2} + \frac{\sqrt{3}}{2}e^{-3\eta^2 t/2} \right) \\ &\times \left\{ \left[\theta_3(e^{-t/\sqrt{3}})\theta_3(e^{-t\sqrt{3}}) - 1 - \frac{\pi}{t} \right] + \left[\theta_2(e^{-t/\sqrt{3}})\theta_2(e^{-t\sqrt{3}}) - \frac{\pi}{t} \right] \right\}. \end{aligned} \quad (59)$$

The total energy per particle E is given by the sum of (55) and (59). The Poisson formula (10) enables us to reduce the integral range to $[0, \pi]$,

$$\begin{aligned} \frac{E(\eta)}{e^2\sqrt{n}} &= \frac{1}{4\sqrt{\pi}} \int_0^\pi \frac{dt}{\sqrt{t}} \left\{ \left(1 - \frac{1}{2}e^{-\eta^2 t/2} + \frac{\sqrt{3}}{2}e^{-3\eta^2 t/2} \right) \left[\theta_3(e^{-t/\sqrt{3}})\theta_3(e^{-t\sqrt{3}}) - 1 - \frac{\pi}{t} \right] \right. \\ &+ \left(1 - \frac{1}{2}e^{-(\pi\eta)^2/(2t)} + \frac{\sqrt{3}}{2}e^{-3(\pi\eta)^2/(2t)} \right) \left[\theta_3(e^{-t/\sqrt{3}})\theta_3(e^{-t\sqrt{3}}) - 1 - \frac{\pi}{t} \right] \\ &+ \left(1 - \frac{1}{2}e^{-\eta^2 t/2} + \frac{\sqrt{3}}{2}e^{-3\eta^2 t/2} \right) \left[\theta_2(e^{-t/\sqrt{3}})\theta_2(e^{-t\sqrt{3}}) - \frac{\pi}{t} \right] \\ &\left. + \left(1 - \frac{1}{2}e^{-(\pi\eta)^2/(2t)} + \frac{\sqrt{3}}{2}e^{-3(\pi\eta)^2/(2t)} \right) \left[\theta_4(e^{-t/\sqrt{3}})\theta_4(e^{-t\sqrt{3}}) - 1 \right] \right\}. \end{aligned} \quad (60)$$

In terms of the functions

$$\begin{aligned} I_2(x, y) &\equiv \int_0^\pi \frac{dt}{\sqrt{t}} e^{-xt/\pi^2} e^{-y\pi^2/t} \left[\theta_2(e^{-t/\sqrt{3}})\theta_2(e^{-t\sqrt{3}}) - \frac{\pi}{t} \right] \\ &= 2 \sum_{j=1}^\infty (-1)^j \left[z_{3/2}(x, y + j^2/\sqrt{3}) + z_{3/2}(x, y + j^2\sqrt{3}) \right] + 4 \sum_{j,k=1}^\infty (-1)^j (-1)^k z_{3/2}(x, y + j^2/\sqrt{3} + k^2\sqrt{3}), \end{aligned} \quad (61)$$

$$\begin{aligned} I_3(x, y) &\equiv \int_0^\pi \frac{dt}{\sqrt{t}} e^{-xt/\pi^2} e^{-y\pi^2/t} \left[\theta_3(e^{-t/\sqrt{3}})\theta_3(e^{-t\sqrt{3}}) - 1 - \frac{\pi}{t} \right] \\ &= 2 \sum_{j=1}^\infty \left[z_{3/2}(x, y + j^2/\sqrt{3}) + z_{3/2}(x, y + j^2\sqrt{3}) \right] + 4 \sum_{j,k=1}^\infty z_{3/2}(x, y + j^2/\sqrt{3} + k^2\sqrt{3}) - \pi z_{1/2}(x, y), \end{aligned} \quad (62)$$

$$\begin{aligned} I_4(x, y) &\equiv \int_0^\pi \frac{dt}{\sqrt{t}} e^{-xt/\pi^2} e^{-y\pi^2/t} \left[\theta_4(e^{-t/\sqrt{3}})\theta_4(e^{-t\sqrt{3}}) - 1 \right] \\ &= 4 \sum_{j,k=1}^\infty z_{3/2}(x, y + (j-1/2)^2/\sqrt{3} + (k-1/2)^2\sqrt{3}) - \pi z_{1/2}(x, y), \end{aligned} \quad (63)$$

the energy per particle E is expressible as

$$\begin{aligned} \frac{E(\eta)}{e^2\sqrt{n}} &= \frac{1}{4\sqrt{\pi}} \left\{ \left[2I_3(0, 0) - \frac{1}{2}I_3((\pi\eta)^2/2, 0) - \frac{1}{2}I_3(0, \eta^2/2) + \frac{\sqrt{3}}{2}I_3(3(\pi\eta)^2/2, 0) + \frac{\sqrt{3}}{2}I_3(0, 3\eta^2/2) \right] \right. \\ &+ \left[I_2(0, 0) - \frac{1}{2}I_2((\pi\eta)^2/2, 0) + \frac{\sqrt{3}}{2}I_2(3(\pi\eta)^2/2, 0) \right] + \left[I_4(0, 0) - \frac{1}{2}I_4(0, \eta^2/2) + \frac{\sqrt{3}}{2}I_4(0, 3\eta^2/2) \right] \left. \right\}. \end{aligned} \quad (64)$$

B. Transition between phases IV and V

Increasing η from η_3^c , phase IV is stable up to the point η_4^c at which the energy of phase IV (46), evaluated at δ^* which minimizes this energy, equals to the energy of phase V (64). Our result is

$$\eta_4^c = 0.73242 \dots \quad (65)$$

The values of η_4^c obtained in the previous studies were relatively dispersed: 0.732,¹⁸ 0.70²⁰ and 0.87.²²

The phase transition is of first order since the energies of phases IV and V have as functions of η different slopes which causes the discontinuity of the first derivative of the energy with respect to η at the transition point η_4^c . The angle parameter δ , which minimizes the energy of the phase IV at the critical point η_4^c , is found to be $\delta^c = 0.69334 \dots$. Since $\delta = \tan(\varphi/2)$, the corresponding angle $\varphi^c = 69.4702 \dots^\circ$; this angle is very close to the estimate $\varphi^c = 69.48^\circ$ of the work.¹⁸ Going from phase IV to V, the angle skips to 60° as is indicated in Fig. 7.

C. Discussion

Two different “sum-rules” can be derived, that allow for a critical assessment of the results obtained. The simplest one relies on the geometrical proximity between structures I (a single hexagonal crystal) and V (two hexagonal crystals at half density). For large distances, the two crystals decouple and we have, making use of straightforward notations,

$$E_I(\sqrt{3}, \eta = 0) = \sqrt{2} E_V(\eta \rightarrow \infty). \quad (66)$$

With our series representations (24) for E_I and (64) for E_V , this identity holds. Another more subtle constraint follows from a combination of elementary geometric considerations,³⁵ which impose that

$$E_V(\eta = 0) = \frac{1 + \sqrt{3}}{2\sqrt{2}} E_I(\sqrt{3}, \eta = 0). \quad (67)$$

We have also checked that this identity holds with the expressions provided above (note though that $\eta = 0$ lies outside the stability range of structure V).

Finally, it is interesting to consider both the large small and large distance behavior of the energy. For small η , it can be shown that both structures I and II share the same energy expansion, up to order η^3 included:

$$E_{II}(\Delta^*, \eta) = E_I(\eta) + \mathcal{O}(\eta^4) \quad (68)$$

where Δ^* is the previously introduced optimal aspect ratio that minimizes $E_{II}(\Delta^*, \eta)$ for a given η . Explicit calculation up to order η^2 shows that

$$\frac{E_{II}(\Delta^*, \eta)}{e^2 \sqrt{n}} = \frac{E_{II}(\sqrt{3}, 0)}{e^2 \sqrt{n}} + \frac{\pi \eta}{\sqrt{2}} - 2.59372 \dots \eta^2 + \mathcal{O}(\eta^3), \quad (69)$$

where the precise value of $E_{II}(\sqrt{3}, 0) = E_I(0)$ has been given in Eq. (25). We note that the linear term in (69) generates a contact pressure $-2\pi\sigma^2 e^2$ for $\eta \rightarrow 0$. A similar term was reported in,¹⁸ where however the term in η^2 differs from ours by a large factor (0.2122 instead of 2.5937)

At large distances, the relevant phase is structure V, from which the inter-plate pressure follows. The large η case is encoded in the small t limit of Eq. (60), or equivalently, Eq. (59). A saddle point argument leads to

$$\frac{E_V(\eta)}{e^2 \sqrt{n}} \sim \frac{E_V(\infty)}{e^2 \sqrt{n}} - \frac{3^{5/4}}{4} \exp\left(-\frac{4\pi}{\sqrt{2} 3^{1/4}} \eta\right). \quad (70)$$

We recover an expression already obtained in,¹⁸ at variance with other approaches.¹⁷ Taking the η derivative and remembering that $n = 2\sigma$ yields the inter-plate pressure

$$P = -2\sigma \frac{\partial E_V}{\partial d} = -2\sigma^{3/2} \frac{\partial E_V}{\partial \eta} \sim -6\pi(\sigma e)^2 \exp\left(-\frac{4\pi}{\sqrt{2} 3^{1/4}} \eta\right). \quad (71)$$

The η dependence is well known, since it can be written $\exp(-G_0 d)$, with G_0 the modulus of the first reciprocal lattice vector. It should be noted though that the prefactor differs from the often reported $2\pi(\sigma e)^2$ (see e.g.¹⁰), by a factor 3.

V. CONCLUSION

The system of classical charged particles, forming a sequence of bilayer Wigner structures at zero temperature as the distance between the plates is increasing, has a rather long history. We have presented here a new method to calculate the Coulomb ground-state energy of each Wigner structure. Based on a series of transformations and using

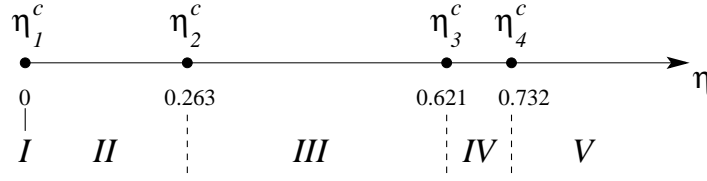


FIG. 8. Summary of phase transition scenario. The rounded off values of the thresholds are mentioned. Structure I is realized at $\eta = 0$ only (vanishing inter-plate separation).

general properties of the Jacobi theta functions, we expressed the energies in terms of quickly converging series of the functions $z_\nu(x, y)$ defined in (22). The presence of the neutralizing background manifests itself simply as the subtraction of singularities of the Jacobi theta functions under an auxiliary integration.

Numerical evaluation of the series requires modest computer and programming facilities, and at the same time provides extremely accurate estimates of the energy. We took advantage of this feature, supplemented by analytical work, to improve and complete previous studies in three aspects:

- There was a relatively large dispersion in the determination of the transition points between phases; this concerns especially the first-order phase transition between phases IV and V. Our method improves significantly the location of all transition points, that can be worked out with arbitrary precision. Figure 8 gives an overview of the sequence of phases together with the corresponding thresholds.
- We resolved, analytically and numerically, a previous controversy about the stability phase I, thereby corroborating the findings of Ref.²¹ We found that this phase is stable only at zero distance between the plates, $\eta = 0 = d$. To confirm numerically this result, we worked with extremely small values of the energy differences $\propto 10^{-12} - 10^{-8}$ for distances $\eta = 10^{-3}$ and 10^{-2} (see Fig. 2), which are “invisible” by standard numerical methods. The agreement between the $\eta \rightarrow 0$ asymptotic relation (32), calculated analytically by using the Taylor expansions of the functions $z_\nu(x, y)$, and the numerical minimization of the energy, presented in Fig. 3, is excellent.
- The expansions of the structure energies around second-order transition points can be done analytically which enables us to specify the critical phenomena at the phase transition points; see the expansions pertaining to the transitions from phase II to III (37) and from phase III to IV (51). The agreement between these analytic formulas and numerical minimization of the ground-state energy is very good; It can be appreciated in Figs. 4 and 6. Quite expectedly for a zero temperature situation, the critical behavior is always of the Ginzburg-Landau type, with the mean-field critical index $\beta = 1/2$ for the growth of the order parameters in the “ordered” phases.

It is clear that our method can be directly generalized to other problems concerning the lattice summations over pair interactions, not only the Coulomb ones. The bilayers with repulsive Yukawa interactions, extensively studied in the past,^{9,21} or with inverse power laws,³⁶ deserve our attention. We additionally emphasize that the ground states under consideration here are such that the ions are distributed evenly (50% on each plate): in other words, the ionic surface density of one Wigner crystal on a given plate is σ , and coincides with the plate homogeneous surface density. When dealing with asymmetric plates, this local neutrality assumption should be relaxed,^{37,39} still enforcing global neutrality. This makes the asymmetric problem significantly more complex, and an interesting perspective for future work. Finally, consideration of dielectric jumps between the walls and the interstitial slab is also a relevant venue for forthcoming investigations.

ACKNOWLEDGMENTS

We would like to thank M. Mazars and C. Texier for useful discussions. L. Š. is grateful to LPTMS for their kind hospitality. The support received from the grants VEGA No. 2/0049/2012 and CE-SAS QUTE is acknowledged.

APPENDIX

The prefactor functions $f_1(\eta)$ and $f_2(\eta)$ of the expansion (29) read

$$f_1(\eta) = \frac{1}{2^{3/2}\sqrt{\pi}} \left\{ 4 \sum_{j=1}^{\infty} j^2 \left[z_{5/2}(0, j^2\sqrt{3}) - \frac{1}{3} z_{5/2}(0, j^2/\sqrt{3}) \right] + 8 \sum_{j,k=1}^{\infty} \left(k^2 - \frac{j^3}{3} \right) z_{5/2}(0, j^2/\sqrt{3} + k^2\sqrt{3}) \right\}$$

$$\begin{aligned}
& +2 \sum_{j=1}^{\infty} (-1)^j j^2 \left[z_{5/2}((\pi\eta)^2, j^2\sqrt{3}) - \frac{1}{3} z_{5/2}((\pi\eta)^2, j^2/\sqrt{3}) \right] \\
& +4 \sum_{j,k=1}^{\infty} (-1)^j (-1)^k \left(k^2 - \frac{j^2}{3} \right) z_{5/2}((\pi\eta)^2, j^2/\sqrt{3} + k^2\sqrt{3}) \\
& +4 \sum_{j,k=1}^{\infty} \left[\left(k - \frac{1}{2} \right)^2 - \frac{1}{3} \left(j - \frac{1}{2} \right)^2 \right] z_{5/2}(0, \eta^2 + (j-1/2)^2/\sqrt{3} + (k-1/2)^2\sqrt{3}) \Bigg\}, \tag{A1}
\end{aligned}$$

$$\begin{aligned}
f_2(\eta) = & \frac{1}{2^{3/2}\sqrt{\pi}} \Bigg\{ 4 \sum_{j=1}^{\infty} \left[\frac{j^4}{2} z_{7/2}(0, j^2\sqrt{3}) + \frac{j^4}{18} z_{7/2}(0, j^2/\sqrt{3}) - \frac{j^2}{3^{3/2}} z_{5/2}(0, j^2/\sqrt{3}) \right] \\
& +8 \sum_{j,k=1}^{\infty} \left[\frac{1}{2} \left(k^2 - \frac{j^3}{3} \right)^2 z_{7/2}(0, j^2/\sqrt{3} + k^2\sqrt{3}) - \frac{j^2}{3^{3/2}} z_{5/2}(0, j^2/\sqrt{3} + k^2\sqrt{3}) \right] \\
& +2 \sum_{j=1}^{\infty} (-1)^j \left[\frac{j^4}{2} z_{7/2}((\pi\eta)^2, j^2\sqrt{3}) + \frac{j^4}{18} z_{7/2}((\pi\eta)^2, j^2/\sqrt{3}) - \frac{j^2}{3^{3/2}} z_{5/2}((\pi\eta)^2, j^2/\sqrt{3}) \right] \\
& +4 \sum_{j,k=1}^{\infty} (-1)^j (-1)^k \left[\frac{1}{2} \left(k^2 - \frac{j^3}{3} \right)^2 z_{7/2}((\pi\eta)^2, j^2/\sqrt{3} + k^2\sqrt{3}) - \frac{j^2}{3^{3/2}} z_{5/2}((\pi\eta)^2, j^2/\sqrt{3} + k^2\sqrt{3}) \right] \\
& +4 \sum_{j,k=1}^{\infty} \left[\frac{1}{2} \left[\left(k - \frac{1}{2} \right)^2 - \frac{1}{3} \left(j - \frac{1}{2} \right)^2 \right]^2 z_{7/2}(0, \eta^2 + (j-1/2)^2/\sqrt{3} + (k-1/2)^2\sqrt{3}) \right. \\
& \left. - \frac{1}{3^{3/2}} \left(j - \frac{1}{2} \right)^2 z_{5/2}(0, \eta^2 + (j-1/2)^2/\sqrt{3} + (k-1/2)^2\sqrt{3}) \right] \Bigg\}. \tag{A2}
\end{aligned}$$

The prefactor function $g_2(\eta)$ of the expansion (33) takes the form

$$\begin{aligned}
g_2(\eta) = & \frac{1}{\sqrt{2\pi}} \Bigg\{ 2 \sum_{j=1}^{\infty} [j^4 z_{7/2}(0, j^2) - j^2 z_{5/2}(0, j^2)] \\
& +2 \sum_{j,k=1}^{\infty} [(j^2 - k^2)^2 z_{7/2}(0, j^2 + k^2) - (j^2 + k^2) z_{5/2}(0, j^2 + k^2)] \\
& + \sum_{j=1}^{\infty} (-1)^j [j^4 z_{7/2}((\pi\eta)^2, j^2) - j^2 z_{5/2}((\pi\eta)^2, j^2)] \\
& + \sum_{j,k=1}^{\infty} (-1)^j (-1)^k [(j^2 - k^2)^2 z_{7/2}((\pi\eta)^2, j^2 + k^2) - (j^2 + k^2) z_{5/2}((\pi\eta)^2, j^2 + k^2)] \\
& + \sum_{j,k=1}^{\infty} \left([(j-1/2)^2 - (k-1/2)^2]^2 z_{7/2}(0, \eta^2 + (j-1/2)^2 + (k-1/2)^2) \right. \\
& \left. - [(j-1/2)^2 + (k-1/2)^2] z_{5/2}(0, \eta^2 + (j-1/2)^2 + (k-1/2)^2) \right) \Bigg\}. \tag{A3}
\end{aligned}$$

Finally, the prefactor function $h_2(\eta)$ of the expansion (47) can be written

$$\begin{aligned}
h_2(\eta) = & \frac{1}{2\sqrt{\pi}} \Bigg\{ 2 \sum_{j=1}^{\infty} [j^4 z_{7/2}(0, j^2) - j^2 z_{5/2}(0, j^2)] + \sum_{j=1}^{\infty} (-1)^j [j^4 z_{7/2}(0, j^2) - j^2 z_{5/2}(0, j^2)] \\
& +2 \sum_{j,k=1}^{\infty} [(j^2 - k^2)^2 z_{7/2}(0, j^2 + k^2) - (j^2 + k^2) z_{5/2}(0, j^2 + k^2)] \\
& + \sum_{j,k=1}^{\infty} (-1)^j (-1)^k [(j^2 - k^2)^2 z_{7/2}(0, j^2 + k^2) - (j^2 + k^2) z_{5/2}(0, j^2 + k^2)] \Bigg\}
\end{aligned}$$

$$\begin{aligned}
& + \sum_{j,k=1}^{\infty} \left([(j-1/2)^2 - (k-1/2)^2]^2 z_{7/2}(0, (j-1/2)^2 + (k-1/2)^2) \right. \\
& - [(j-1/2)^2 + (k-1/2)^2] z_{5/2}(0, (j-1/2)^2 + (k-1/2)^2) \Big) \\
& + \sum_{j=1}^{\infty} [j^4 z_{7/2}((\pi\eta)^2/2, j^2) - j^2 z_{5/2}((\pi\eta)^2/2, j^2)] + \sum_{j=1}^{\infty} (-1)^j [j^4 z_{7/2}((\pi\eta)^2/2, j^2) - j^2 z_{5/2}((\pi\eta)^2/2, j^2)] \\
& + 2 \sum_{j,k=1}^{\infty} (-1)^j [(j^2 - k^2)^2 z_{7/2}((\pi\eta)^2/2, j^2 + k^2) - (j^2 + k^2) z_{5/2}((\pi\eta)^2/2, j^2 + k^2)] \\
& + \sum_{j=1}^{\infty} [(j-1/2)^4 z_{7/2}(0, \eta^2/2 + (j-1/2)^2) - (j-1/2)^2 z_{5/2}(0, \eta^2/2 + (j-1/2)^2)] \\
& + 2 \sum_{j,k=1}^{\infty} \left([(j-1/2)^2 - k^2]^2 z_{7/2}(0, \eta^2/2 + (j-1/2)^2 + k^2) \right. \\
& \left. - [(j-1/2)^2 + k^2] z_{5/2}(0, \eta^2/2 + (j-1/2)^2 + k^2) \right) \Big\}. \tag{A4}
\end{aligned}$$

* On leave from Institute of Physics, Slovak Academy of Sciences, Bratislava, Slovakia

- ¹ E. Wigner, Phys. Rev. **46**, 1002 (1934).
- ² C.G. Grimes and G. Adams, Phys. Rev. Lett. **42**, 795 (1979).
- ³ D.V. Fil, Low Temp. Phys. **27**, 384 (2001); Y.P. Chen, Phys. Rev. B **73**, 115314 (2006); Z. Wang, Y.P. Chen, L.W. Engel, D.C. Tsui, E. Tutuc, and M. Shayegan, Phys. Rev. Lett. **99**, 136804 (2007).
- ⁴ H. Imamura, P. A. Maksym and H. Aoki, Phys. Rev. B **53**, 12 613 (1996).
- ⁵ R. M. Ribeiro and N. M. R. Peres, Phys. Rev. B **83**, 235312 (2011).
- ⁶ T. B. Mitchell, J. J. Bollinger, D. H. E. Dubin, X.-P. Huang, W. M. Itano, B. M. Baughman, Science **282**, 1290 (1998).
- ⁷ L. Teng and P. Tu, L. I, Phys. Rev. Lett. **90**, 245004 (2003).
- ⁸ S. Naser, C. Bechinger, P. Leiderer and T. Palberg, Phys. Rev. Lett. **79**, 2348 (1997).
- ⁹ M. Mazars, Physics Reports **500**, 43 (2011).
- ¹⁰ A. W. C. Lau, D. Levine, and P. Pincus, Phys. Rev. Lett. **84**, 4116 (2000). A.W.C. Lau, P. Pincus, D. Levine, and H.A. Fertig, Phys. Rev. E **63**, 051604 (2001).
- ¹¹ A.Y. Grosberg, T.T. Nguyen, and B.I. Shklovskii, Rev. Mod. Phys. **74**, 329 (2002).
- ¹² Y. Levin, Rep. Prog. Phys. **65**, 1577 (2002).
- ¹³ A. Naji, S. Jungblut, A.G. Moreira, and R.R. Netz, Physica A **352**, 131 (2005).
- ¹⁴ L. Šamaj and E. Trizac, Phys. Rev. Lett. **106**, 078301 (2011); Phys. Rev. E **84**, 041401 (2011).
- ¹⁵ L. Šamaj and E. Trizac, Contrib. Plasma Phys. **52**, 53 (2012).
- ¹⁶ V.I. Falko, Phys. Rev. B **49**, 7774 (1994).
- ¹⁷ K. Esfarjani and Y. Kawazoe, J. Phys.: Condens. Matter **7** 7217 (1995).
- ¹⁸ G. Goldoni and F.M. Peeters, Phys. Rev. B **53**, 4591 (1996).
- ¹⁹ I. V. Schweigert, V. A. Schweigert, and F. M. Peeters, Phys. Rev. Lett. **82**, 5293 (1999); Phys. Rev. B **60**, 14 665 (1999).
- ²⁰ J.J. Weis, D. Levesque, and S. Jorge, Phys. Rev. B **63**, 045308 (2001).
- ²¹ R. Messina and H. Löwen, Phys. Rev. Lett. **91**, 146101 (2003); E.C. Oğuz, R. Messina, and H. Löwen, Europhys. Lett. **86**, 28002 (2009).
- ²² V. Lobaskin and R.R. Netz, Europhys. Lett. **77**, 38003 (2007).
- ²³ L. Bonsall and A. A. Maradudin, Phys. Rev. B **15**, 1959 (1977).
- ²⁴ E. A. Jagla, J. Chem. Phys. **110**, 451 (1999).
- ²⁵ M. Abramowitz and I. A. Stegun (Eds.), Handbook of Mathematical Functions with Formulas, Graphs, and Mathematical Tables, 9th printing, New York: Dover (1972).
- ²⁶ L. D. Landau and E. M. Lifshitz, Statistical Physics, Course of Theoretical Physics vol 5, Pergamon Press (1980).
- ²⁷ L. Šamaj and E. Trizac, to appear in EPL (2012).
- ²⁸ S. W. de Leeuw, J. W. Perram and E. R. Smith, Proc. R. Soc. Lond. A, **373**, 27 (1980).
- ²⁹ I. S. Gradshteyn and I. M. Ryzhik, *Table of Integrals, Series, and Products*, 6th edn (Academic Press, London, 2000).
- ³⁰ R.D. Misra, Proc. Camb. Phil. Soc. **36**, 173 (1940).
- ³¹ M. Born and R.D. Misra, Proc. Camb. Phil. Soc. **36**, 466 (1940).
- ³² D. Borwein, J.M. Borwein, R. Shail, and I.J. Zucker, J. Phys. A: Math. Gen. **21**, 1519 (1988).
- ³³ M.J. Bowick, A. Cacciuto, D.R. Nelson, and A. Travesset, Phys. Rev. B **73**, 024115 (2006).

- ³⁴ This value is fully consistent with that reported in Refs.^{18,23} In addition, it also provides us with the Madelung constant of the hexagonal Wigner crystal on a single charged plate $M = -E(\sqrt{3}, 0)/(e^2\sqrt{n\pi}) \simeq 1.106103$, as can be found in Refs.^{12,38}.
- ³⁵ I. Rouzina and V.A. Bloomfield, J. Phys. Chem. **100**, 9977 (1996).
- ³⁶ M. Mazars, J. Phys. A: Math. Theor. **43**, 425002 (2010).
- ³⁷ R. Messina, C. Holm, and K. Kremer, Phys. Rev. Lett. **85**, 872 (2000). R. Messina, C. Holm and K. Kremer, Europhys. Lett. **51**, 461 (2000).
- ³⁸ B. I. Shklovskii, Phys. Rev. E **60**, 5802 (1999).
- ³⁹ R. Messina, J. Phys.: Condens. Matter **21** 113102 (2009).